Analysis of the synergistic effect on the strength characteristics of modified red mud-based stabilized soil

Chen Shengjin * , Jiang Jie , Ou Xiaoduo , Tan Zhijie

Posted Date: 13 July 2023

doi: 10.20944/preprints202307.0942.v1

Keywords: stabilized soil; red mud; synergistic effect; nano-SiO2; strength characteristics

Article

Analysis of the Synergistic Effect on the Strength Characteristics of Modified red Mud-Based Stabilized Soil

Chen Shengjin [1], Ou Xiaoduo [2,*], Jiang Jie [2] and Tan Zhijie [1]

[1] Guangxi Hualan Geotechnical Engineering Co., Ltd, Nanning, Guangxi 530001;
[2] Guangxi University, Nanning, Guangxi 530004
3 Correspondence: Ou Xiaoduo, ouxiaoduo@163.com

Abstract: In order to effectively utilize red mud, an aluminum industrial waste, the stabilized soil material was developed using nano-SiO_2 synergistically modified red mud, and the strength characteristics of the stabilized soil were analyzed to clarify the feasibility of such stabilized soil serves as a road base material. Through different combination schemes, the effects of different nano-SiO_2 and cement contents on the strength of the stabilized materials were explored. The test results show that: in the synergistic modification of nano-SiO_2 and cement, nano-SiO_2 can significantly improve the early unconfined compressive strength of red mud-based stabilized soil; in the synergistic modification of nano-SiO_2, gypsum and cement, the 7-d unconfined compressive strength of red mud-based stabilized soil is greater than 2 MPa, which meets the strength requirements of road base materials and shows the superiority of synergism. The nominal stress-strain curves are divided into five stages: compressed and compacted stage, elastic deformation stage, plastic deformation stage, damage deformation stage and residual deformation stage. The macroscopic compressive damage pattern of the specimens shows that the modified red mud-based stabilized soil mostly exhibits brittle damage.

Keywords: stabilized soil; red mud; synergistic; nano-SiO_2; strength characteristics

1. Introduction

Red mud is a solid waste generated during alumina production (Wang et al., 2020; Xue et al. 2016a), and its utilization rate is extremely low (Xie et al., 2020). With the increase in alumina production capacity worldwide, large amounts of red mud are generated every year (Liao et al., 2019; Zhu et al., 2016a), and red mud requires large amounts of land for stockpiling, which has a huge impact on both the natural environment and land resources (Bombik et al., 2020; Lockwood et al., 2015). Reducing red mud piles and promoting the resourceful use of red mud are important issues affecting the development of the aluminum industry.

The key to solving environmental problems in red mud disposal is to develop technologies that can directly consume large quantities of red mud or convert it into a secondary resource for reuse. Currently, in the engineering field, red mud is mainly used in the manufacture of bricks and ceramics, or as a raw material for cement and road base material (Li et al., 2022; Atan et al., 2021; Zhao et al., 2021). Ou et al., (2022) blended red mud with bauxite tailings and cement with different mass ratios to develop new road base materials, and the results showed that the 7-day unconfined compressive strength was 3.03 MPa at a ratio of red mud to bauxite tailings of 2:1, which met the strength requirements of low-grade roads of class II and below. Ma et al., (2022) used red mud as an additive for loess, and the results showed that adding appropriate amounts of red mud will promote the production of hydration products and effectively improve the unconfined compressive strength and shear strength of the treated loess. Mukiza et al., (2019) investigated the possibility of using red mud as road base material, soft subsoil stabilizer and road base material. It was found that the performance of red mud as road base material was superior to that of natural soil, and the synergistic use of red mud and other wastes also improved the mechanical and durability properties of the material compared to the use of red mud alone. This literature shows clearly that scholars have promoted the

 doi:10.20944/preprints202307.0942.v1

application of red mud reduction by using red mud as a major or partial raw material in engineering practice. And red mud serves as a base material in road base filling has also shown great potential. It is expected that the use of red mud-based materials in this field can greatly benefit the process of red mud reduction.

Nano-SiO_2 has a high specific surface area and good volcanic ash activity in alkaline environments, which can accelerate the hydration of nano-SiO_2-cement systems to form complex micro-structured C-S-H gels to improve early strength (Gayathiri et al., 2022; Lin et al., 2022; Kumar et al., 2021; Nandhini et al., 2021). Meanwhile, it was proved that Nano-SiO_2 can play a role in the reuse of red mud. Ahmed et al., (2020) added nano-SiO_2 in the synthesis of a geopolymer binder with red mud as the main solid source and found that the addition of suitable levels of nano-SiO_2 contributed to the formation of geopolymer gels and C-S-H, thus giving geopolymer with higher compressive strength. The relevant literature shows that nano-SiO_2 has obvious performance advantages and can play a great role in civil engineering. However, there is few researches on how to utilize the advantages of nano-materials in red mud modification for strength improvement. Therefore, in this paper, nano-SiO_2 is synergistically involved in the modification of red mud-based stabilized soil to study the effect of nano-SiO_2 on strength improvement of red mud-based stabilized soil. A series of unconfined compression test were conducted on the red mud-based stabilized specimens with different nano-SiO_2, cement and gypsum contents. Based on the experimental results, the strength characteristics of stabilized soil materials are analyzed.

2. Materials and Methods

2.1. Raw materials

2.1.1. Red mud

The red mud used was Bayer red mud, taken from an aluminum company in Guangxi Provice. The specific gravity of the tested red mud was 3.06. The natural moisture content of the red mud was in the range of 28.10%~35.21%.

According to the Standard for soil test method (GB/T50123-2019), the particle composition of red mud was tested by densitometry method. The particle analysis curve of the test red mud is shown in Figure 1. It shows that the content of particles with particle size less than 0.075 mm is 97.8%, while the content of particles with particle size less than 0.01 mm is 63.6%, so the red mud is a kind of fine-grained soil.

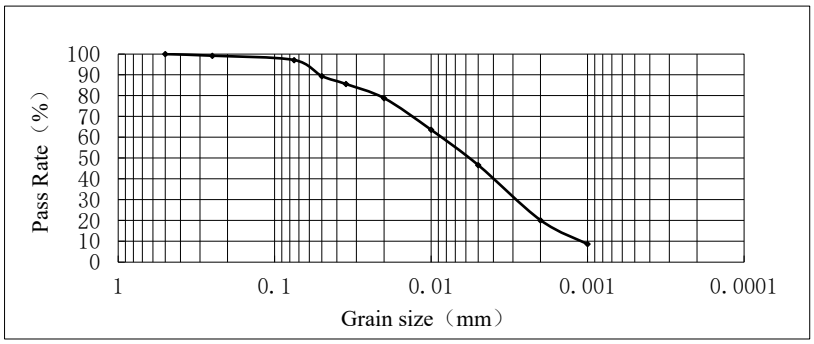

Figure 1. Particle gradation curve of the tested red mud.

2.1.2. Nano-SiO_2

The selected nano-SiO_2 was produced by mechanical crushing process. The nano-SiO_2 is a white spherical powder with 99.9% purity. Its particle size ranges between 1 and 100 nm. The specific surface area of the nano-SiO_2 particle is 240 m^2 /g.

Preprints (www.preprints.org) | NOT PEER-REVIEWED | Posted: 13 July 2023 doi:10.20944/preprints202307.0942.v1

2.1.3. Cement

The cement used for the test was 42.5 grade ordinary silicate cement with a specific surface area of 340 m^2 /kg and a density of 3.10 g /cm^3.

2.1.4. Gypsum

The gypsum chosen for the experiment is a kind of construction gypsum. It is a white powder with a density of 2.32 g/cm^3, and its chemical formula is $CaSO_4$-0.5H_2O.

2.2. Experimental design

In combination with the studies of Wang et al. (2020), Wang et al. (2019) and Li et al. (2019), nano-SiO_2 was incorporated into the red mud-based stabilized soil at mass ratio of 0.5%, 1%, 1.5%, 2%, 2.5% and 3%; gypsum was incorporated into the red mud-based stabilized soil at 6% of mass ratio; and cement was incorporated into the red mud-based stabilized soil at 1%, 3%, 5%, 7% and 9% by mass.

The test procedure was as follows:

① Adding cement alone to dry red mud and testing the effect of the individual admixture of cement on the strength of the specimen;
② The nano-SiO_2 dosing of 1% was selected to test the effect of different cement dosing on the unconfined compressive strength of specimens under the synergistic effect of nano-SiO_2;
③ The optimum dose of 3% cement and 6% gypsum was selected from both strength and economic considerations, and different mass ratios of nano-SiO_2 were added on this basis to test the synergistic effects of the three modified materials on strength control, and to determine the optimum nano-SiO_2 dosage.

The synergistic combination scheme of the experimental design is shown in Table 1, where, RM is red mud; NS, PC and CS are the abbreviations of nano-SiO_2, cement and gypsum, respectively; the following number refers to the blending mass ratios of corresponding materials (%).

Table 1. Collaborative combination scheme table.

Projects	Synergistic Solution Portfolio				
	Program 1	**Program 2**	**Program 3**	**Program 4**	**Program 5**
RM unmodified	RM				
PC individually modified	PC1	PC3	PC5	PC7	PC9
NS+PC synergistic modification	NS1PC1	NS1PC3	NS1PC5	NS1PC7	NS1PC9
NS+CS6+PC3 synergistic modification	NS0.5CS6PC3	NS1CS6PC3	NS2CS6PC3	NS3CS6PC3	

2.3. Specimen preparation

The stabilized soil with different sterilizers as shown in Table 1 were compacted into cylindrical specimens of 50 mm × 50 mm (Figure 2) as per the Test Method of Materials Stabilized whit Inorganic Binders for Highway Engineering (JTG E51-2009) and Liu et al. (2018).

Preprints (www.preprints.org) | NOT PEER-REVIEWED | Posted: 13 July 2023 doi:10.20944/preprints202307.0942.v1

Figure 2. Photographs of cylindrical specimens.

The specimen preparation and curing steps are as followings:

① Firstly, the sampling red mud was dried at room temperature and crushed into powder with a plastic hammer; then the crushed powder was sieved using a 0.5 mm steel sieve; the sieved red mud was oven-dried at 105°C to further remove the moisture.

② According to the optimal water content determined by the compaction test, the modified materials (stabilizers, all in powder form) and certain mass of deionized water were added into the red mud according to the designed dosage and mixed thoroughly.

③ The stabilized soil was compacted to a 5mm×5mm cylindrical column. Note that the compaction should be done within 1 hour after adding cement.

④ The compacted specimens were sealed with plastic film and placed in an environmentally-controlled chamber with temperature of 20°C and a relative humidity of 95° for curing. After reaching different curing periods of 1, 7, 14, 28, 60 and 120 days, the specimens were taken out for unconfined compressive strength test.

2.4. Unconfined compressive strength test

The unconfined compression test was carried out by TSZ series fully automatic triaxial instrument produced by Nanjing Soil Instrument Factory Co. The instrument can directly obtain the experimental maximum compressive strength and the relationship curve between the main stress difference and axial strain. The experimental parameters were set as follows: specimen height: 5 cm; specimen diameter: 5 cm; rigid steel ring coefficient: 30 N/mm; axial strain: 15%; loading level: 1 level; sampling step: 0.125 mm; shear rate: 2.5 mm/min.

Once the experiment was started, the instrument can automatically collect the compressive strength data and generate the stress-strain curve simultaneously until the specimen is completely damaged and loses its compressive capacity. Figure 3 shows the damaged state of the tested specimen.

Preprints (www.preprints.org) | NOT PEER-REVIEWED | Posted: 13 July 2023 doi:10.20944/preprints202307.0942.v1

Figure 3. Specimen damage by compression.

The unconfined compressive strength is calculated according to Equation 1:

$$q_u = \frac{P}{A} \quad (1)$$

where, q_u is compressive strength of the specimen (MPa), accurate to 0.01 MPa; P is the breaking load of the specimen (N); A is the pressure-bearing area of the specimen (mm^2).

3. Results and analysis

3.1. Effect of cement

When the cement was modified alone, the specimens were dosed with 1%, 3%, 5%, 7% and 9% of cement. The test results are shown in Figure 4.

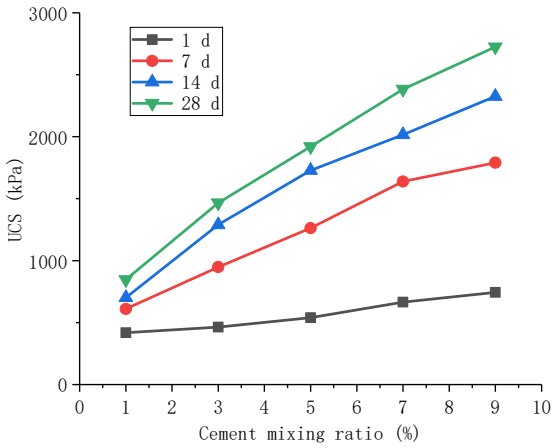

Figure 4. Effect of cement on UCS.

Figure 4 shows that the unconfined compressive strength at 7 d is 491 kPa, 928 kPa, 1262 kPa, 1639 kPa and 1797 kPa for 1%, 3%, 5%, 7% and 9% of cement admixture, respectively, and the unconfined compressive strength increases to 437 kPa, 334 kPa, 377 kPa and 152 kPa for each 2% increase of cement, indicating that the increase of cement admixture can lead to higher unconfined compressive strength of the red mud-based stabilized soil.

The unconfined compressive strength of cement-modified red mud-based stabilized soil increased with the increase of the curing time, and the unconfined compressive strengths of cement with 3% admixture are 463, 948, 1289 and 1466 kPa at 1, 7, 14 and 28 d, respectively., with the growth values of the first 7 and 28 d compressive strengths accounting for 48.3% and 82.3% of the growth values of the 28 d compressive strength.

3.2. Effect of synergistic modification

3.2.1. Effect of nano-SiO_2 and cement co-modification

The increase in the unconfined compressive strength of the red mud-based stabilized soil was tested by adding 1% nano-SiO_2 with the cement admixture still at 1%, 3%, 5%, 7%, and 9% and the nano-SiO_2 in cooperation with the cement. The test results are shown in Figure 5 and Figure 6.

Figure 5 shows that the unconfined compressive strength of the red mud-based stabilized soil modified by nano-SiO_2 co-cement showed a linear increase with the increase of cement admixture, for example, the unconfined compressive strength at 7d was 865, 1434, 1892, 2273 and 2547 kPa for

Preprints (www.preprints.org) | NOT PEER-REVIEWED | Posted: 13 July 2023 doi:10.20944/preprints202307.0942.v1

1%, 3%, 5%, 7% and 9% of cement admixture, respectively For each 2% increase of cement, the increases were 569, 458, 381 and 274 kPa, respectively.

The unconfined compressive strength of the red mud-based stabilized soil modified with nano-SiO_2 co-cement increased with the increase of the curing time, but the growth rate of the unconfined compressive strength was significantly greater when the curing time increased from 1 d to 7 d than when the curing time increased from 7 d to 14 d and from 14 d to 28 d. The growth rate of the unconfined compressive strength of the red mud-based stabilized soil modified with nano-SiO_2 co-cement increased with the increase of the curing time.

Figures 6 show the comparison of unconfined compressive strength with curing time for the addition of 1% nano-SiO2 with and without the addition of nano-SiO2, provided that the cement admixture is 3%. The NS1PC3 combination of nano-SiO2 synergistically modified with cement showed a large increase in unconfined compressive strength with curing time.. For the same curing age, the unconfined compressive strength of the NS1PC3 synergistically modified combination increased by 27.7%, 51.2%, 54.5% and 56.1%, respectively, compared to the PC3 alone modified combination. In addition to this, there is a characteristic that the growth of the lateral limit compressive strength tends to increase from 1 to 7d, and the subsequent growth is more moderate, indicating that the growth rate of the lateral limit compressive strength is mainly concentrated from 1 to 7d. This indicates that the synergistic effect of nano-SiO_2 and cement improves the early unconfined compressive strength of the red mud-based stabilized soil.

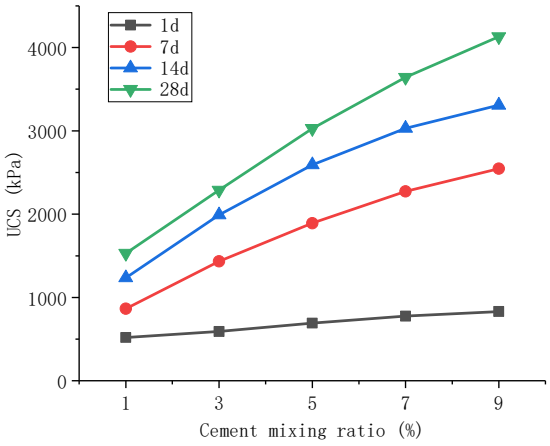

Figure. 5. Effect of nano-SiO_2 and cement on UCS

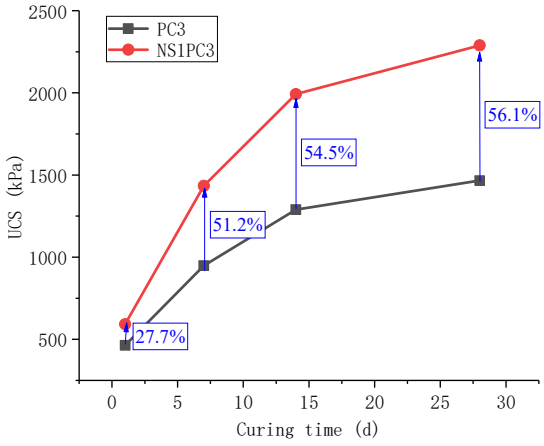

Figure. 6. Comparison of UCS of NS1PC3 and PC3

3.2.2. Effect of nano-SiO_2 co-modification with cement and gypsum

Under the premise of 3% of cement and 6% of gypsum, nano-SiO_2 was selected at 0.5%, 1%, 2% and 3% to test the increase of unconfined compressive strength of red mud-based stabilized soil under the action of nano-SiO_2 in cooperation with cement and gypsum. The test results are shown in Figure 7.

It can be found that when the curing time was 7 d, the unconfined compressive strengths of nano-SiO_2 with 0.5%, 1%, 2% and 3% doping were 2421, 2748, 2467 and 2156 kPa, respectively. The unconfined compressive strength did not increase with the increase of nano-SiO_2 doping, and the highest strength was achieved with the combination of nano-SiO_2 with 1% doping. Referring to the Technical Guidelines for Construction of Highway Roadbases (JTG/T F20-2015), the 7 d unconfined compressive strength of red mud base stabilized soil is required to reach 2 MPa.

In contrast, the unconfined compressive strength of the modified red mud-based stabilized soil increased with the increase of the curing time, and the growth rate of the unconfined compressive strength was the largest in the curing age of 7 d. The growth value of compressive strength in the first 7 d accounted for 69.2% of the growth value of compressive strength at 28 d, based on the nano-SiO_2 dosing of 1%. Figure 7 also show that the highest unconfined compressive strength was obtained for the

Preprints (www.preprints.org) | NOT PEER-REVIEWED | Posted: 13 July 2023 doi:10.20944/preprints202307.0942.v1

combination of gypsum and cement involved in the synergistic modification at 1% of nano-SiO_2. The 7 d unconfined compressive strength of NS1CS6PC3 reached 2748 kPa, which meets the strength requirements as a general road stabilized soil, and the cement dosing was not the highest for the selected combination, also considering the economic requirements, which is the optimal combination from the strength point of view. The next best combination is NS2CS6PC3.

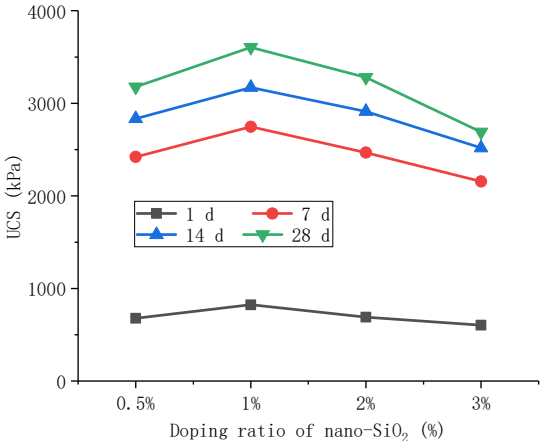

Figure 7. Effect of nano-SiO2 doping on the lateral limit compressive strength of the synergistic combination of gypsum and cement.

3.2.3. Analysis of the synergistic effect of nano-SiO_2

In this section, the synergistic modification characteristics of nano-SiO_2, gypsum and cement will be analyzed, focusing on the synergistic effect of nano-SiO_2.

The 7 d unconfined compressive strength results of the gypsum and cement dosing for the optimal combination determined in the test, i.e., at 6% gypsum and 3% cement, for the corresponding combinations with and without nano-SiO_2, were tabulated and analyzed, as shown in Table 2.

Table 2. UCS of stabilized specimens containing nano-SiO_2 (unit: kPa).

Projects	NS doping							Remarks
	0	0.5%	1%	1.5%	2%	2.5%	3%	
RM unmodified	388							Control test
PC3 separately modified	948							
NS1+PC3 synergistic modification			1434					
NS+CS6+PC3 synergistic modification		2421	2748		2467		2156	

The analysis of the synergistic effects of the involvement of nano-SiO_2 before and after modification concluded that:

(1) When the red mud is unmodified, the unconfined compressive strength of the specimens made under the conditions of 93% compaction, optimum moisture content and maximum dry density is 388 kPa, which has a structural strength, but because no modified material is added, the unconfined compressive strength cannot be enhanced with the increase of curing time, and at the same time, the structure of the compacted specimens will be damaged if disturbed by external forces.

(2) Cement modification alone can make the red mud-based stabilized soil obtain higher compressive strength than that of unmodified, and the 7-d unconfined compressive strength with 3% cement admixture is 948 kPa, which is about 2.5 times of that of unmodified compressive specimens. When 1% of nano-SiO_2 was added, the compressive strength of the red mud-based stabilized soil reached 1434 kPa, which was 1.5 times of the compressive strength of the red mud-based stabilized soil modified by PC3 alone. The synergistic effect of nano-SiO2 promoted the modification of the red mud-based stabilized soil and led to further growth of the lateral-free compressive strength.

Preprints (www.preprints.org) | NOT PEER-REVIEWED | Posted: 13 July 2023 doi:10.20944/preprints202307.0942.v1

(3) When nano-SiO_2 was modified with CS6 and PC3, the modified red mud-based stabilized soil obtained higher unconfined compressive strength, and the 7 d unconfined compressive strength obtained at 1% of nano-SiO_2 was 2748 kPa, which was greater than the strength of 591 kPa of NS1 modified with CS6 and 1434 kPa of NS1 modified with PC3, and greater than the sum of 2025 kPa. This value is greater than the strength of NS1 modified soil with CS6 of 591 kPa and the strength of NS1 modified soil with PC3 of 1434 kPa, and is greater than the sum of both of them of 2025 kPa. The synergistic effect of nano-SiO_2 with CS and PC has obtained the effect of "1+1>2".

(4) The above series of unconfined compressive strength tests gradually revealed the optimal amount of the three modified materials, while further revealing the superiority of the synergistic effect to enhance the compressive strength of the modified materials, and NS1CS6PC3 was the best modified solution for the test from both economic and strength considerations.

3.3. Compressive damage characteristics of red mud-based stabilized soil

3.3.1. Nominal stress-strain relationship

Figure 8 shows the nominal stress-strain curves of the red mud-based stabilized soil under compression for each modification condition.

Figure 8 show that the nominal stress-strain curves of the red mud-based stabilized soil under compression under each modification condition exhibit elastic-plastic deformation, which can be roughly divided into five stages according to the curve morphology, and the curve morphology of each stage varies under different modification conditions. The stress-strain curves of the combined specimens of nano-SiO_2 , gypsum and cement synergistically modified at the age of 28 d are used to label the stage division.

In the first stage, OA section, the slope of the stress-strain curve increases continuously and is concave, but the course is short. The analysis suggests that the specimen is formed in this stage because the pore ratio under pressure becomes smaller, the specimen soil particles and the modified materials not involved in the reaction are further compacted, and the stiffness increases, resulting in the increasing compressive strength. This stage belongs to the "compacted stage", and the shape of the curve of the red mud-based stabilized soil is basically the same in this stage under each modification condition.

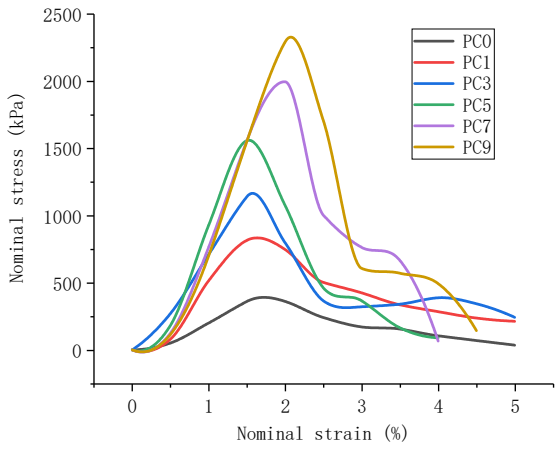

(a) Nominal stress-strain curve of cement-modified specimens at 28d age

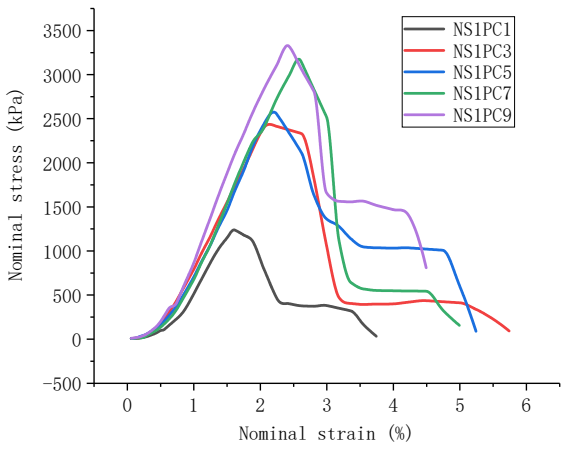

(b) Nominal stress-strain curves of specimens modified with SiO_2 and cement at 28d.

Preprints (www.preprints.org) | NOT PEER-REVIEWED | Posted: 13 July 2023 doi:10.20944/preprints202307.0942.v1

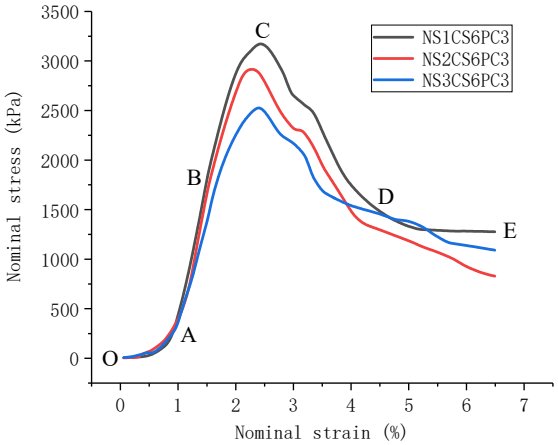

(c) Nominal stress-strain curves of specimens modified with nano-SiO_2, gypsum and cement at the age of 28d

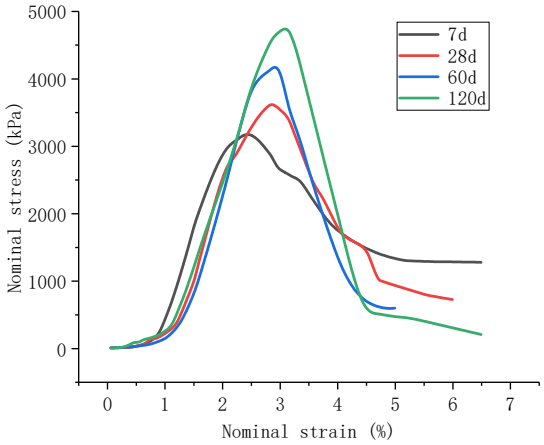

(d) Nominal stress-strain curve of NS1CS6PC3 modified combination with curing time

Figure 8. Nominal stress-strain relationship curve of modified red mud-based stabilized soil

In the second stage, AB section, the stress-strain relationship curve in this stage is approximately linear, and the nominal stress of the red clay-based stabilized soil increases linearly with the increase of the nominal strain, and this stage is the "elastic deformation stage", and the stress corresponding to the B point is the proportional limit. The shape of the second stage is slightly different under different modification conditions, but in general, the higher the compressive strength is, the higher the B point is in the stress rise stage. As shown in Figure 8 (a) and Figure 8 (b), the higher the PC doping, the higher the B point, Figure 8 (c), the highest B point at 1% of nano-SiO_2, while Figure 8 (d) shows that the higher the age of curing, the higher the B point. In the elastic deformation stage, the red clay-based stabilized soil resists the load through the cohesion and friction between the material particles, and the nominal strain and stress further increase with the progressive increase of the load one, but it has not yet exceeded the material resistance, so the deformation cracks have not yet appeared in the specimens at this stage.

The third stage, BC section, the slope of the stress-strain curve in this section is decreasing, the shape of the curve is concave, the stress reaches the peak and then stops growing, the peak stress, i.e., the corresponding stress at point C is the unconfined compressive strength of the test material, this stage is the "plastic deformation stage" of the test material, which is also the "yielding stage". stage". In this stage, after the stress exceeds the proportional limit, the strain increases significantly with the increase of stress, and the terracotta stabilized soil softens, resulting in microcracks in the test material, which are mainly parallel to the loading direction, and then with the further increase of load, the microcracks in the specimen also increase and gradually extend and expand, and the duration of this process is relatively short. reversible damage, but the curve pattern shows that the specimen material can still withstand the increased load until the stress reaches the peak. When the stress state reaches the peak, a fall occurs, which is caused by the continuous development of microcracks through the development of the material load bearing capacity decreases and destabilization, and finally enters the fourth stage - the damage deformation stage.

The fourth stage, CD section, after the curve crosses the peak from point C, the nominal stress decreases sharply with the increase of strain, this stage is the "damage deformation stage" of the material, also similar to the second stage, the curve shape is slightly different under different modification conditions, in general, the higher the strength of the material, the more rapidly the stress decay, such as PC alone For example, the higher the PC dose, the higher the rate of decline of the curve for the red clay-based stabilized soil modified by PC alone, and the greater the rate of decline of the curve for the red clay-based stabilized soil modified by NS1CS6PC3, the greater the rate of decline of the curve at this stage with the increase of the curing age, showing the characteristics of

 doi:10.20944/preprints202307.0942.v1

"brittle damage". In the "damage deformation stage" of the material, the cracks of the red clay-based stabilized soil penetrate the top and bottom of the specimen, and the cracks keep increasing, and the material strain of the specimen softens and destabilizes, leading to the rapid decay of the material resistance.

The fifth stage, DE section, this stage is the "residual deformation stage" of the test material, in this stage, the specimens produce a lot of plastic deformation, terracotta-based stabilized soil after the destruction of the stress does not disappear completely, and even some specimens still retain a small value, the strength is the residual strength, but with the increase in stress, the nominal stress will eventually tend to zero. The compressive specimens of each modified red clay-based stabilized soil also roughly show two different characteristics at this stage, most of them have a stress "damage platform", and after the "damage platform" the nominal stress decays rapidly again, and a few of them do not have a "damage platform", and the stress gradually decays. breaking platform", the stress gradually decreases. For example, in the case of the red mud-based stabilized soil specimen modified by cement alone, the higher the PC admixture, the higher the unconfined compressive strength, and the "breaking platform" is shown in the fifth stage, where the nominal stress does not continue to decay but appears to "stagnate" with strain growth The nominal stresses decayed rapidly again and tended to zero until the end of the test; the stress-strain curves of NS1PC modified red clay-based stabilized soil showed the characteristics of "damage plateau" in all specimens at this stage, with the difference that NS1CS6PC3 modified red clay-based stabilized soil, the nominal stress did not show the plateau effect when the curing age was short, but when the curing age reached 120 d, the plateau effect was obvious. The platform effect is obvious when the curing age reaches 120d. In general, the "damage plateau" was more obvious in the specimens with high unconfined compressive strength for the same modified red clay-based stabilized soil.

The ratio of residual stress to peak stress is shown in Table 3. The ratio of residual stress to peak stress decreases with the growth of the curing age, showing the development from plastic to elastic.

Table 3. Ratio of residual stress to peak stress.

Curing period (d)	0	14	28	60	120
Residual stress/peak stress	0.53	0.44	0.24	0.16	0.13

From the above analysis, it can be seen that the red mud-based stabilized soil has different deformation mechanisms during uniaxial compression. During the compressive compacting stage, the material mainly shows that the pore ratio becomes smaller, the material particles are further compacted, and the compressive strength is further enhanced; in the elastic stage, the material particle compactness continues to be strengthened, and the external load is resisted through the cohesion and friction between particles, and when the external load is continuously increased, the resistance of the material is continuously enhanced, but the material still does not appear cracks; in the plastic stage, the material appears micro-cracks and gradually extend and expand, and then form penetration cracks, and irreversible damage occurs, but the material is not destabilized and damaged, and the compressive strength can still increase with the increase of external load, and reaches the peak before the material destabilization and damage, and there is an obvious strain softening behavior of the material; in the damage stage, the cracks keep increasing, and accompanied by the specimen fragment body falling off from the main body of the specimen, and the material resistance decays rapidly, but before the compressive capacity completely disappears Before the complete loss of compressive capacity, most of the specimens showed the ductility characteristics of increasing stress invariant stress, indicating that the red mud-based stabilized soil has good buffering performance and still has certain bearing capacity after the damage. Finally, with the increase of compressive time, the specimens were finally completely destabilized and destroyed.

Preprints (www.preprints.org) | NOT PEER-REVIEWED | Posted: 13 July 2023 doi:10.20944/preprints202307.0942.v1

3.3.2. Typical damage characteristics

Figure 9 shows the typical damage pattern of the red mud-based stabilized soil specimen under compression.

(a) Typical damage pattern of red mud-based stabilized soil without modified materials under pressure

(b) Typical damage pattern of red mud-based stabilized soil with modified materials under pressure

(c) Lateral and top surface morphology of red mud-based stabilized soil with modified materials after compression damage

(d) Internal morphology of red mud-based stabilized soil with modified materials after compression damage

Figure 9. Typical damage pattern of red mud-based stabilized soil under pressure

Figure 9 (a) shows the compression damage pattern of the pure red clay-based stabilized soil, which shows the typical plastic damage under the uniaxial compression condition. The cracks are continuously developed upward and finally penetrate to the top of the specimen until the specimen is completely destroyed, and the bottom bulge also causes the cracks to be wide at the bottom and thin at the top. Figure 8 (a) shows that, the nominal stress-strain curve of the PC0 specimen shows that the peak stress is relatively small, but the nominal strain is not the smallest, which also reaches 4.5%.

Figure 9 (b) shows the typical damage pattern of red clay-based stabilized soil under compression after the addition of modified materials. Most of the modified red clay-based stabilized soil shows brittle damage, especially when the modified materials and the curing age promote the increase of nominal stress, the brittle damage characteristics are more obvious. Under the load, the specimens did not show bulging phenomenon, under the condition of increasing uniaxial pressure, the specimens began to show fine cracks along the direction of loading, the cracks also started to appear from the bottom, but would penetrate quickly from bottom to top (Figure 9 (c)), local

specimens would show oblique cracks, but vertical cracks were dominant. In the stage of damage deformation, the cracks keep increasing, the specimen bottom appears local slip, and the penetration cracks cut the specimen into several pieces, at the same time, the outer layer of the specimen appears to fall off due to cracking.. When the strain increases, transverse cracks appear on part of the side, and the transverse cracks promote the shear damage of the side, combined with the stress-strain curve analysis, this time "damage platform" When the side without transverse shear damage is also damaged, the "damage platform" in the stress-strain curve is crossed and enters the final sharp decay of the stress, and finally the stress tends to zero due to the complete destruction of the specimen (Figure 9 (d)).

4. Conclusions

In this experiment, the stabilized soil material was prepared by modifying the red mud from aluminum industrial waste, and the strength characteristics of the red mud-based stabilized soil with different modified materials and different amounts of modified materials were tested and analyzed, and the main findings were as follows:

(1) Cement alone can improve the unconfined compressive strength of red mud-based stabilized soil; when nano-SiO2 is modified with cement, nano-SiO2 can significantly improve the early unconfined compressive strength of red mud-based stabilized soil; when nano-SiO_2, gypsum and cement are modified with 6% gypsum and 3% cement, under the synergistic effect of nano-SiO_2 (1%, 2% and 3%, respectively), the unconfined compressive strength of red mud-based The 7d unconfined compressive strength of the stabilized soil was greater than 2 MPa, and the maximum was achieved at 1% of nano-SiO2. The synergistic results of the addition of nano-SiO_2, and gypsum and cement showed the superiority of synergy.

(2) The compressive deformation of the red mud-based stabilized soil shows the characteristics of elastic-plastic deformation, and the nominal stress-strain curves of the red mud-based stabilized soil under each modified condition are divided into five stages: "compressive compacting stage", "elastic deformation and plastic deformation stage", "damage deformation and residual deformation stage", and so on, "Most of the specimens showed "damage platform". Most of the specimens showed the ductility characteristics of increasing stress before the compressive capacity completely disappeared, indicating that the red mud-based stabilized soil has good buffering performance.

（3）The compressive damage morphology of the specimens showed that the modified red mud-based stabilized soil exhibited mostly brittle damage. Under the condition of increasing uniaxial pressure, vertical cracks appeared in the specimens first, and with the increase of cracks, slip appeared at the bottom. When the pressure kept increasing, the specimens showed transverse cracks and finally the specimens were completely destroyed.

References

[1] Ahmed S, Meng T, Taha M. Utilization of red mud for producing a high strength binder by composition optimization and nano strengthening [J]. Nanotechnology Reviews, 2020, 9(1):396-409.

[2] Atan E, Sutcu M, Cam A S. Combined effects of bayer process bauxite waste (red mud) and agricultural waste on technological properties of fired clay bricks [J]. Journal of Building Engineering, 2021, 43(3):103194.

[3] Bombik E, Bombik A, Rymuza K.The influence of environmental pollution with fluorine compounds on the level of fluoride in soil, feed and eggs of laying hens in Central Pomerania, Poland[J].Environmental Monitoring and Assessment, 2020, 192(3).

[4] Gayathiri K, Praveenkumar S. Influence of Nano Silica on Fresh and Hardened Properties of Cement-based Materials – A Review [J]. 2022, Silicon:1-31.

[5] GB/T50123-2019, Standard for soil test method [S]. Beijing:China Planning Press, 2019.

[6] JTG/T F20-2015, Technical Guidelines for Construction of Highway Roadbases [S]. Beijing:Ministry of Transport of the People's Republic of China, 2015.

[7] JTG E51-2009, Test Method of Materials Stabilized whit Inorganic Binders for Highway Engineering [S]. Beijing:People's Traffic Publishing House, 2009.

[8] Kumar D P, Amit S, Chand M. Influence of various nano-size materials on fresh and hardened state of fast

setting high early strength concrete [FSHESC]: A state-of-the-art review [J]. Construction and Building Materials, 2021, 277(1):122299.

[9] Liao S Z, Yang J L, Ma S J, et al. Research Progress in the Comprehensive Utilization of Red Mud [J]. Conservation and Utilization of Mineral Resources, 2019.

[10] Li X F, Guo Y, Zhu F, et al. Alkalinity stabilization behavior of bauxite residue: Ca-driving regulation characteristics of gypsum [J]. Journal of Central South University, 2019, 26(2):383-392.

[11] Li Z F, Gao Y F, Zhang M, et al. The enhancement effect of Ca-bentonite on the working performance of red mud-slag based geopolymeric grout [J]. Materials Chemistry and Physics, 2022, Volume 276(35): 125311.

[12] Lin R S, Seokhoon Oh, Du W, et al. Strengthening the performance of limestone-calcined clay cement (LC3) using nano silic [J]. Construction and Building Materials, 2022, 340:127723.

[13] Liu S, Li Z, Li Y, et al. Strength properties of Bayer red mud stabilized by lime-fly ash using orthogonal experiments [J]. Construction and Building Materials, 2018, 166:554-563.

[14] Lockwood, C.L.; Stewart, D.I.; Mortimer, R.; Mayes, W.M.; Jarvis, A.P.; Gruiz, K.; Burke, I.T. Leaching of copper and nickel in soil-water systems contaminated by bauxite residue (red mud) from Ajka, Hungary: The importance of soil organic matter. Environ. Sci. Pollut. Res. 2015, 22, 10800–10810.

[15] Ma Q W, Duan W, Liu X F, et al. Engineering Performance Evaluation of Recycled Red Mud Stabilized Loessial Silt as a Sustainable Subgrade Material [J]. Materials, 2022, 9:3391.

[16] Mukiza E, Zhang L L, Liu X, et al. Utilization of red mud in road base and subgrade materials: A review [J]. Resources, Conservation and Recycling, 2019, 141:187-199.

[17] Nandhini K, Ponmalar V. Effect of Blending Micro and Nano Silica on the Mechanical and Durability Properties of Self-Compacting Concrete [J]. Silicon, 2021, 13(3):687–695.

[18] Ou X D, Chen S J, Jiang J, et al. Reuse of Red Mud and Bauxite Tailings Mud as Subgrade Materials from the Perspective of Mechanical Properties [J]. Materials, 2022, 15(3):1123.

[19] Wang J B, Du P, Zhou H Z, et al. Effect of nano-silica on hydration, microstructure of alkali-activated slag [J]. Construction and Building Materials, 2019, 220(30):110-118.

[20] Wang S, Jin H, Deng Y, et al. Comprehensive utilization status of red mud in China: A critical review [J]. Journal of Cleaner Production, 2020, 289(11):125136.

[21] Wang Y G, Geng Y F, Zhang HM, et al. Effect of nano-silica on alkaline slag cement flooding[J]. Silicate Bulletin, 2020, 39(05):1451-1456+1465.(In Chinese)

[22] Xue S G, Kong X F, Zhu F, et al. 2016a． Proposal for management and alkalinity transformation of bauxite residue in China [J]． Environmental Science and Pollution Research， 23 (13): 12822-12834.

[23] Xie W, Zhou F, Liu J, et al. Synergistic reutilization of red mud and spent pot lining for recovering valuable components and stabilizing harmful element [J]. Journal of Cleaner Production, 2020, 243(Jan.10):118624.1-118624.12.

[24] Zhao H, Gou H. Unfired bricks prepared with red mud and calcium sulfoaluminate cement: Properties and environmental impact [J]. Journal of Building Engineering, 2021, 38(7):102238.

[25] Zhu F，Li Y B，Xue S G，et al． 2016a． Effects of iron-aluminium oxides and organic carbon on aggregate stability of bauxite residues [J]． Environmental Science and Pollution Research，23 (9) : 9073-9081.